

# ATP-induced helicase slippage reveals highly coordinated subunits

Bo Sun<sup>1,2\*</sup>, Daniel S. Johnson<sup>1,2,†\*</sup>, Gayatri Patel<sup>3</sup>, Benjamin Y. Smith<sup>1,2</sup>, Manjula Pandey<sup>3</sup>, Smita S. Patel<sup>3</sup> & Michelle D. Wang<sup>1,2</sup>

Helicases are vital enzymes that carry out strand separation of duplex nucleic acids during replication, repair and recombination<sup>1,2</sup>. Bacteriophage T7 gene product 4 is a model hexameric helicase that has been observed to use dTTP, but not ATP, to unwind double-stranded (ds)DNA as it translocates from 5' to 3' along single-stranded (ss)DNA<sup>2-6</sup>. Whether and how different subunits of the helicase coordinate their chemo-mechanical activities and DNA binding during translocation is still under debate<sup>1,7</sup>. Here we address this question using a single-molecule approach to monitor helicase unwinding. We found that T7 helicase does in fact unwind dsDNA in the presence of ATP and that the unwinding rate is even faster than that with dTTP. However, unwinding traces showed a remarkable sawtooth pattern where processive unwinding was repeatedly interrupted by sudden slippage events, ultimately preventing unwinding over a substantial distance. This behaviour was not observed with dTTP alone and was greatly reduced when ATP solution was supplemented with a small amount of dTTP. These findings presented an opportunity to use nucleotide mixtures to investigate helicase subunit coordination. We found that T7 helicase binds and hydrolyses ATP and dTTP by competitive kinetics such that the unwinding rate is dictated simply by their respective maximum rates  $V_{\max}$ , Michaelis constants  $K_M$  and concentrations. In contrast, processivity does not follow a simple competitive behaviour and shows a cooperative dependence on nucleotide concentrations. This does not agree with an uncoordinated mechanism where each subunit functions independently, but supports a model where nearly all subunits coordinate their chemo-mechanical activities and DNA binding. Our data indicate that only one subunit at a time can accept a nucleotide while other subunits are nucleotide-ligated and thus they interact with the DNA to ensure processivity. Such subunit coordination may be general to many ring-shaped helicases and reveals a potential mechanism for regulation of DNA unwinding during replication.

Despite the fact that most motor proteins use ATP as a fuel source, previous bulk studies have shown that T7 helicase does not unwind DNA efficiently in the presence of ATP, although it is capable of ATP hydrolysis<sup>5,6,8</sup>. To investigate why ATP seemed not to support T7 helicase unwinding, we used a single-molecule optical trapping assay that we previously developed to measure unwinding of dsDNA or translocation on ssDNA (Fig. 1a and Supplementary Fig. 1)<sup>9</sup>. Briefly, two strands of a DNA fork junction were held under tension that was not sufficient to mechanically unwind the junction without a helicase. Helicase unwinding of the junction resulted in an increase in the ssDNA length, permitting tracking of the helicase location. When experiments were conducted with 2 mM ATP, we were surprised to find that ATP supported not only dsDNA unwinding but that it also supported it at a significantly faster rate than with dTTP (Fig. 1b–c). However, processive unwinding was interrupted by slippage events, resulting in a remarkable sawtooth pattern in the unwinding trace

(Fig. 1b). Control experiments verified that each trace was the action of a single helicase (Supplementary Fig. 2). We attribute this pattern to helicase losing its grip on the ssDNA, sliding backwards under the influence of the reannealing DNA fork, and then regaining its grip and resuming unwinding (Fig. 1d). In contrast, slippage behaviour was essentially absent with 2 mM dTTP alone (Fig. 1b). These results resolve the mystery of the apparent lack of significant unwinding activity seen in bulk studies<sup>4-6,8</sup>; unwinding and slippage could not be separated, so unwinding was masked by unobservable slips that prevented helicase from moving over a substantial distance. Our work is the first direct observation, to our knowledge, of helicase nucleotide-specific slippage. Previous studies of non-ring-shaped helicases have reported reverse motions of the unwinding fork attributable to helicase reaching the end of the DNA or encountering a barrier<sup>10,11</sup>, dissociating from the DNA<sup>12,13</sup>, or moving in the reverse direction<sup>9,12,13</sup>. These are of a somewhat different nature than what we have observed. The only slippage behaviour that may resemble ours is from non-helicase bacteriophage motors<sup>14,15</sup>, but their slippage is not a result of the use of a specific nucleotide.

Slippage was not observed with dTTP alone (Fig. 1b) and therefore seems to be sensitive either to the base composition of the bound nucleotide (for example, adenosine versus thymidine) or the type of sugar (ribose versus deoxyribose). We compared slippage for all four NTPs and their dNTP counterparts (Supplementary Fig. 3). For each nucleotide we measured processivity, defined as the mean distance between slips (Supplementary Fig. 4). The results indicate that the additional 2'-OH group on the ribose sugar makes the helicase more prone to slipping. Examination of the helicase structure at the nucleotide-binding pocket<sup>16</sup> reveals that the 2'-OH group of a bound nucleotide may displace the -OH group on the side chain of residue Y535 (Supplementary Fig. 5a). We thus generated a Y535F mutant to remove the -OH group and it showed significantly increased processivity in the presence of ATP, albeit still less than that seen for dATP (Supplementary Fig. 5b).

Although ATP caused helicase to slip more frequently, it supported a much faster unwinding rate between slips, consistent with an earlier finding of a faster rate of ATP hydrolysis<sup>17</sup>. Because ATP and dTTP support different unwinding rates and processivities, we used nucleotide mixtures to understand how multiple subunits of the helicase coordinate unwinding activity. We approximated the *in vivo* concentrations of ATP and dTTP of *Escherichia coli*<sup>18</sup> by using 2.0 mM ATP and a small amount of dTTP, 0.2 mM (Fig. 1b, c). Although the unwinding rate between slips was close to the value observed with 2 mM ATP alone, the processivity increased by approximately threefold. When the converse experiment was performed (0.2 mM ATP and 2.0 mM dTTP), the unwinding rate was comparable to that with 2 mM dTTP alone and minimal slippage was observed (Fig. 1b, c). These results imply that even a small fraction of helicase subunits, when bound with dTTP, reduce slippage and substantially increase processivity. This finding was further substantiated by bulk experiments using ATP alone, and an ATP/dTTP mixture (Supplementary Fig. 6). To determine if T7

<sup>1</sup>Department of Physics - Laboratory of Atomic and Solid State Physics, Cornell University, Ithaca, New York 14853, USA. <sup>2</sup>Howard Hughes Medical Institute, Cornell University, Ithaca, New York 14853, USA.

<sup>3</sup>Department of Biochemistry, UMDNJ-Robert Wood Johnson Medical School, Piscataway, New Jersey 08854, USA. <sup>†</sup>Present address: Rockefeller University, New York, New York 10065, USA.

\*These authors contributed equally to this work.

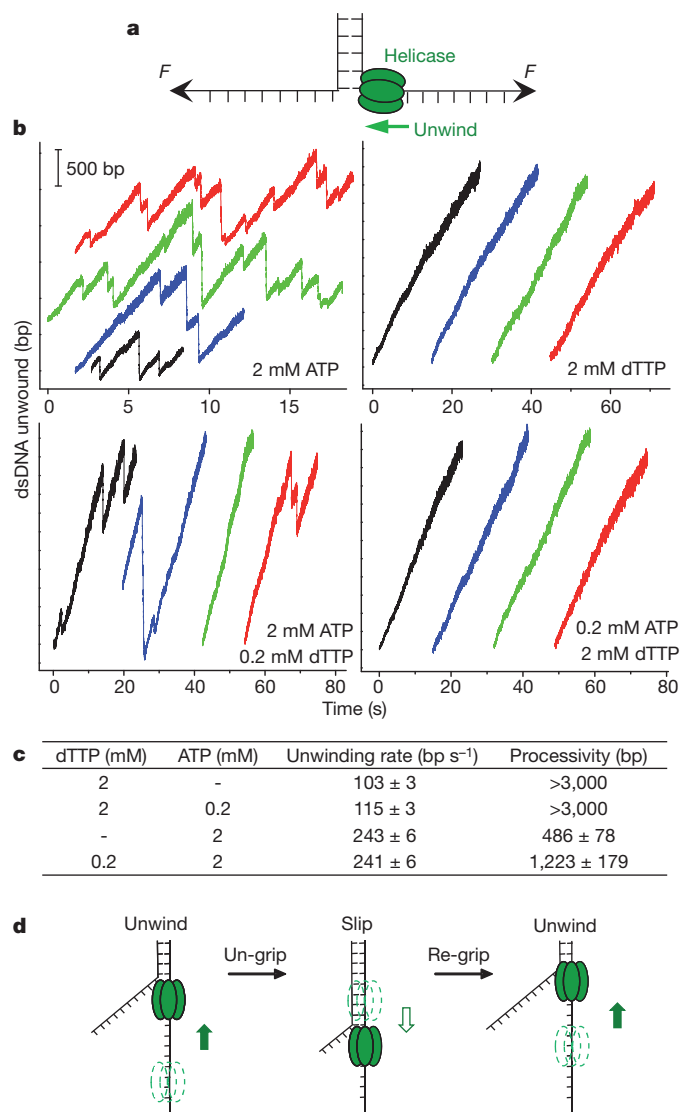


**Figure 1 | Comparison of helicase unwinding behaviours with different nucleotides.** **a**, Schematic of the single-molecule configuration (not to scale). The single-stranded ends of a dsDNA were held at a constant unzipping force of 8 pN while T7 helicase unwound the dsDNA by translocating on ssDNA. **b**, Representative traces showing the number of unwound base pairs versus time in the presence of various concentrations of nucleotides. For clarity, traces have been arbitrarily shifted along both axes. **c**, A summary of unwinding rates and processivities. Uncertainties are s.e.m. **d**, Cartoon illustrating slippage behaviour. The helicase unwinds, loses grip, slips, re-grips and resumes unwinding. Dotted helicase indicates a previous location of the helicase.

helicase binds DNA with different affinities in the presence of dTTP and ATP, bulk binding studies were carried out using fluorescence anisotropy with dTTP and ATP analogues (Supplementary Fig. 7). The results show that T7 helicase binds ssDNA 100-fold more tightly with dTMPPCP than with AMPPCP, and indicate that the greater slippage in the presence of ATP is probably due to weaker binding to DNA.

The discovery of helicase slippage and the ability to directly measure helicase processivity provided a unique opportunity to explore the following: (1) how ATP and dTTP compete for binding to helicase subunits; (2) how nucleotide binding regulates helicase affinity to DNA; and (3) how multiple subunits of helicase coordinate their activities.

To understand how ATP and dTTP compete for binding to helicase subunits, we determined the unwinding rates between slippage events (Fig. 2a) as a function of nucleotide concentration. For each nucleotide alone, the unwinding rate followed Michaelis–Menten-like kinetics, yielding  $V_{\max}$  and  $K_M$  values that were both higher for ATP than for

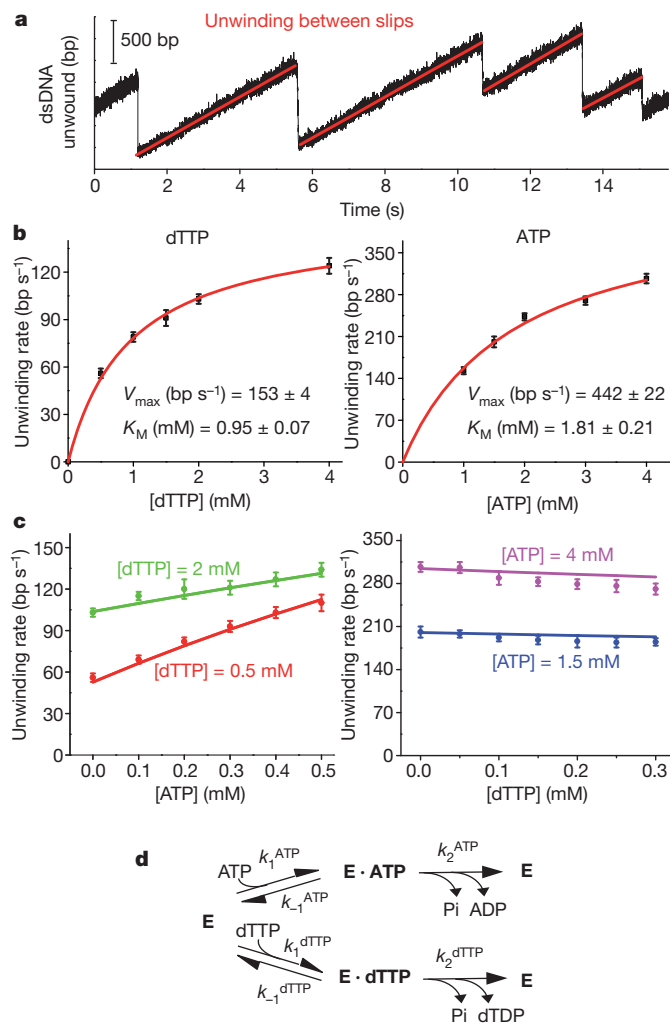


**Figure 2 | Helicase unwinding kinetics.** **a**, Example of unwinding with ATP to illustrate the method of determining unwinding rate by analysing data between slippage events. **b**, Kinetic constants for unwinding under a constant unzipping tension of 8 pN in the presence of either ATP (right) or dTTP (left). For each nucleotide,  $K_M$  and  $V_{\max}$  were obtained by fitting the unwinding rates as a function of NTP concentration to the Michaelis–Menten equation. **c**, Measured unwinding rates at either fixed [dTTP] and varying [ATP], or fixed [ATP] and varying [dTTP], and comparison with direct predictions (not fits) from the competitive nucleotide binding model using kinetic constants  $K_M$  and  $V_{\max}$  shown in **b**. Error bars indicate s.e.m. **d**, Kinetic pathway of a competitive binding model where ATP and dTTP compete for binding and hydrolysis by the helicase (denoted by E here).

dTTP (Fig. 2b). These kinetics indicated that there was no cooperativity in NTP binding and hydrolysis. Next, we conducted experiments in which the concentration of one nucleotide was fixed while that of the other nucleotide was varied. The resulting unwinding rates could be explained by competitive kinetics: ATP and dTTP compete for binding based on their respective affinities and the resulting reaction rate is determined by their concentrations,  $V_{\max}$ , and  $K_M$  (Fig. 2c, d; Methods Summary and Supplementary Discussion). A comparison of unwinding rates with mixed nucleotides and direct predictions (not fits) from the competitive binding kinetics showed excellent agreement. These results were further substantiated by ssDNA translocation rate experiments (Supplementary Fig. 8). This also explains why in Fig. 1b, c the unwinding rate was minimally altered when 0.2 mM of dTTP was added to 2 mM ATP. Under those conditions, only about 16% of the nucleotide bound to the helicase hexamer was dTTP.

The competitive binding kinetics for nucleotides, however, does not explain the observed slippage behaviour with mixed nucleotides (Fig. 1b, c). That is, it is unclear how the 16% bound dTTP resulted

in a threefold increase in processivity. If only a single nucleotide can be bound by the helicase at a time and the type of the bound nucleotide determines the helicase's affinity to the DNA, then processivity should only increase by 7% (Supplementary Discussion). In addition, it has previously been shown that the helicase subunits do not bind to ssDNA in the absence of a nucleotide<sup>19</sup>. However, we found minimal slippage even at [dTTP] much below its  $K_M$ . These observations indicate participation of multiple subunits in both nucleotide and DNA binding, where each subunit would have a nucleotide-specific DNA binding affinity. Our data indicate that helicase may not slip if at least one subunit of the hexamer is in a deoxythymidine-ligated state, which has a higher affinity for the DNA.

Two models may be consistent with this idea. In an uncoordinated model<sup>1,2,7</sup>, each helicase subunit functions independently in its nucleotide binding/hydrolysis, and DNA binding/release (Supplementary Discussion). Conversely, coordinated models have been proposed for T7 helicase<sup>1,2,7</sup>, but details of the coordination remain unclear. Biochemical and structural studies indicate that nucleotide hydrolysis may occur sequentially around the hexameric ring<sup>16,20,21</sup>, that roughly four subunits are nucleotide-ligated at any given time<sup>20</sup>, and that DNA binding to the helicase might involve one-to-two helicase subunits<sup>16,20–22</sup>. A model based on structural studies has been proposed for ring-shaped helicases E1 (ref. 23) and Rho<sup>24</sup>, where all or some of the subunits coordinate their chemo-mechanical activities (Fig. 3d). Coordination

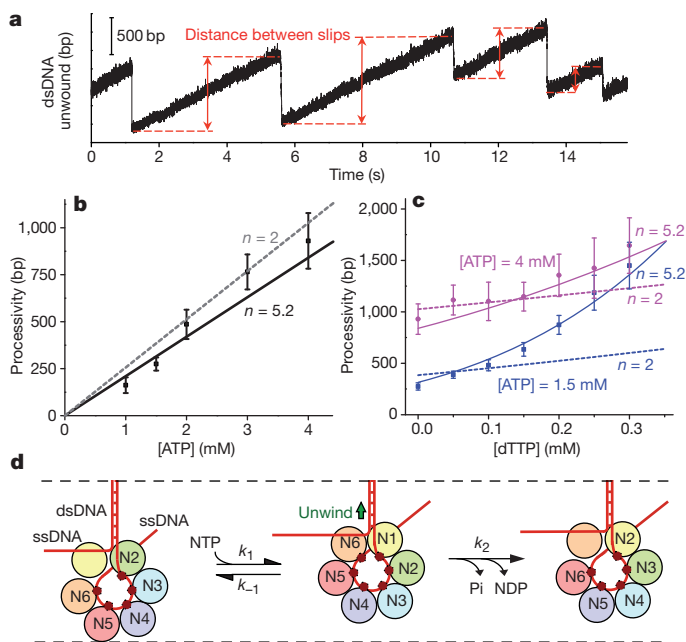


**Figure 3 | Processivity dependence on nucleotides and a proposed coordinated model.** **a**, An example of unwinding with ATP to illustrate the method of determining distance between slips. **b**, **c**, Measured processivity (mean distance between slipping events) as a function of [ATP] alone, and as functions of [dTTP] at two fixed concentrations of ATP. Note processivity increased substantially when a small amount of dTTP was added to the reaction. Solid lines are global fits using the coordinated model, yielding  $n = 5.2 \pm 0.4$ . For comparison, fits using  $n = 2$  are also shown. Error bars indicate s.e.m. **d**, An interpretation of the proposed coordinated model. Each subunit is uniquely labelled with a different colour and has a potential ssDNA-binding site (small red dot). Nucleotide binding and subsequent hydrolysis occur sequentially around the ring. If a subunit is nucleotide-ligated (the state of hydrolysis indicated by  $N_i$ ), it has a non-zero probability of being bound to ssDNA. During unwinding, the leading subunit can bind to a nucleotide (N) and thus acquire affinity to the upstream ssDNA. This stimulates the last nucleotide-bound subunit to release its nucleotide and ssDNA. Then the cycle proceeds again around the ring. Slippage occurs when all subunits simultaneously release ssDNA, as determined by the joint probability of detachment for all subunits (Supplementary Discussion).

could occur sequentially around the hexameric ring with the leading subunit poised for NTP binding and each successive subunit having a bound nucleotide in states of progression along the chemical reaction pathway (NTP, NDP + Pi, NDP, and so on). Depending on the state and type of nucleotide bound each subunit may have a different affinity to DNA. Once the leading subunit binds to an NTP and reels in the DNA, the remaining subunits progress to their next reaction states. Product release by the last participating subunit results in release of DNA from that subunit, and thus completes a single cycle.

We formulated quantitative descriptions for the uncoordinated and coordinated models (Supplementary Discussion). The observed rate of unwinding as a function of [ATP] or [dTTP] is consistent with both models, which predict an apparent Michaelis–Menten-like kinetics. The observed unwinding rate with ATP and dTTP mixtures is also consistent with the competitive binding kinetics for both models as long as, in the case of the coordinated model, the rates are treated as averages over time (Supplementary Discussion). Although the two models cannot be distinguished based on rate measurement studies, they do yield different predictions for DNA slippage behaviour. The uncoordinated model (Supplementary Discussion) requires that each subunit binds and hydrolyses nucleotides independently with an affinity to DNA dependent on the state and type of nucleotide bound. This model is not consistent with the processivity data taken with mixed nucleotides at concentrations near or lower than their respective  $K_M$  values (Supplementary Fig. 9).

On the other hand, the coordinated model requires that subunits participating in coordination bind and hydrolyse nucleotide in coordination, with only one subunit poised to bind a nucleotide at a time and with each subunit having an affinity to DNA dependent on the state and type of nucleotide bound. This model predicts that processivity should increase linearly with [NTP] in the presence of a single type of NTP. Indeed, our data show that the processivity increases linearly with increasing [ATP] (Fig. 3a, b). If multiple helicase subunits coordinate in their chemo-mechanical activities, what is the degree of coordination as measured by the number of participating subunits at any given time ( $n$ )? This is a key parameter that characterizes the mechanism of the helicase. Previous studies indicate that only one or two subunits are involved in significant DNA binding, suggesting a lower degree of coordination of  $n = 1$  or 2 (refs. 16, 20–22). However, subunits may participate in the coordination even if they have lower affinity to ssDNA. The coordinated model formulated (Supplementary Discussion) is rather general and naturally takes this into account. Interestingly, it predicts that processivity sensitively depends on  $n$  as [dTTP] is increased in the presence of a fixed [ATP]—the larger  $n$ , the more subunits participate in DNA binding, and the more steeply processivity increases with [dTTP]. Therefore we measured processivity with mixtures of ATP and dTTP (Fig. 3c). A global fit to the processivity data in Fig. 3b, c yielded  $n = 5.2 \pm 0.4$  (Methods Summary). In contrast,  $n = 2$  does not agree with the measurements. These findings are further substantiated by experiments using UTP instead of ATP (Supplementary Fig. 10,  $n = 5.0 \pm 0.3$ ), experiments under a different unzipping force (Supplementary Fig. 11,  $n = 5.4 \pm 0.3$ ), and data on time between slips (Supplementary Fig. 12,  $n = 5.5 \pm 0.4$ ). Because  $n \leq 6$  is expected for a hexamer, this finding indicates that nearly all subunits participate in the coordination ( $n = 5$  or 6) (Fig. 3d). Our findings suggest that only one subunit at a time can accept an incoming nucleotide, while the rest of the subunits are already nucleotide bound and coordinate to prevent slippage and maintain high processivity.

The work presented here provides a quantitative description of nucleotide binding/hydrolysis and its coupling to DNA binding and translocation for T7 helicase. This was possible because unwinding and slippage events are clearly distinguishable in single-molecule traces. The slippage behaviour is explained by a multiple-site coordinated model. For helicase to slip, all six subunits must simultaneously lose their grip on the DNA. This happens more often when helicase subunits are bound only to ribose nucleotides. Our data demonstrate

that T7 helicase has a very weak DNA binding affinity in the presence of ATP but the addition of a small amount of dTTP to the ATP reaction increases the binding affinity of helicase to DNA. As a consequence, the presence of a single deoxythymidine-ligated subunit significantly decreases the chance of slippage so that helicase can still effectively unwind dsDNA with ATP. Thus T7 helicase, like most other helicases<sup>2</sup>, could still use ATP as a main power source *in vivo*, under conditions such as those during phage infection of *E. coli*<sup>18</sup> where ATP is most abundant. ATP could be used for rapid unwinding and dTTP for high processivity. Although we focus here on a comparison of dTTP with ATP for helicase unwinding, other deoxyribose nucleotides may also reduce the frequency of slippage (Supplementary Fig. 3). We speculate that slippage may also provide an evolutionary advantage for replication: when dNTP concentrations are low, slippage can slow down helicase to allow its synchronization with a slow-moving DNA polymerase.

## METHODS SUMMARY

Single-molecule assays were performed as described previously<sup>9</sup>. If dTTP and ATP compete for binding to helicase according to the kinetic pathway outlined in Fig. 2d, then the resulting unwinding rate is:  $V_{\text{tot}} = \left( V_{\text{max}}^{\text{ATP}} \frac{[\text{ATP}]}{K_{\text{M}}^{\text{ATP}}} + V_{\text{max}}^{\text{dTTP}} \frac{[\text{dTTP}]}{K_{\text{M}}^{\text{dTTP}}} \right) / \left( 1 + \frac{[\text{ATP}]}{K_{\text{M}}^{\text{ATP}}} + \frac{[\text{dTTP}]}{K_{\text{M}}^{\text{dTTP}}} \right)$ , where for each type of nucleotide  $K_{\text{M}} = \frac{k_{-1} + k_2}{k_1}$  and  $V_{\text{max}} = sk_2$  with  $s$  being the step size (in nucleotides) (see Supplementary Discussion). In the presence of dTTP and ATP, if  $n$  helicase subunits coordinate in their chemo-mechanical activities and DNA binding, then the resulting distance between slips (processivity) is:  $d_{\text{processivity}} = c \left( V_{\text{max}}^{\text{ATP}} \frac{[\text{ATP}]}{K_{\text{M}}^{\text{ATP}}} + V_{\text{max}}^{\text{dTTP}} \frac{[\text{dTTP}]}{K_{\text{M}}^{\text{dTTP}}} \right) / \left( \frac{[\text{ATP}]/K_{\text{M}}^{\text{ATP}}}{[\text{ATP}]/K_{\text{M}}^{\text{ATP}} + [\text{dTTP}]/K_{\text{M}}^{\text{dTTP}}} \right)^{n-1}$  (Supplementary Discussion), with  $c$  being a proportionality constant. This expression was used to fit data in Fig. 3b,  $c$  with  $c$  and  $n$  as fit parameters.

**Full Methods** and any associated references are available in the online version of the paper at [www.nature.com/nature](http://www.nature.com/nature).

Received 24 December 2010; accepted 1 August 2011.

Published online 18 September; corrected 6 October 2011 (see full-text HTML version for details).

- Singleton, M. R., Dillingham, M. S. & Wigley, D. B. Structure and mechanism of helicases and nucleic acid translocases. *Annu. Rev. Biochem.* **76**, 23–50 (2007).
- Patel, S. S. & Picha, K. M. Structure and function of hexameric helicases. *Annu. Rev. Biochem.* **69**, 651–697 (2000).
- Donmez, I. & Patel, S. S. Mechanisms of a ring shaped helicase. *Nucleic Acids Res.* **34**, 4216–4224 (2006).
- Matson, S. W., Tabor, S. & Richardson, C. C. The gene 4 protein of bacteriophage T7. Characterization of helicase activity. *J. Biol. Chem.* **258**, 14017–14024 (1983).
- Matson, S. W. & Richardson, C. C. DNA-dependent nucleoside 5'-triphosphatase activity of the gene 4 protein of bacteriophage T7. *J. Biol. Chem.* **258**, 14009–14016 (1983).
- Hingorani, M. M. & Patel, S. S. Cooperative interactions of nucleotide ligands are linked to oligomerization and DNA binding in bacteriophage T7 gene 4 helicases. *Biochemistry* **35**, 2218–2228 (1996).
- Lyubimov, A. Y., Strycharska, M. & Berger, J. M. The nuts and bolts of ring-translocase structure and mechanism. *Curr. Opin. Struct. Biol.* **21**, 240–248 (2011).
- Lee, S. J. & Richardson, C. C. Molecular basis for recognition of nucleoside triphosphate by gene 4 helicase of bacteriophage T7. *J. Biol. Chem.* **285**, 31462–31471 (2010).
- Johnson, D. S., Bai, L., Smith, B. Y., Patel, S. S. & Wang, M. D. Single-molecule studies reveal dynamics of DNA unwinding by the ring-shaped T7 helicase. *Cell* **129**, 1299–1309 (2007).
- Myong, S., Rasnik, I., Joo, C., Lohman, T. M. & Ha, T. Repetitive shuttling of a motor protein on DNA. *Nature* **437**, 1321–1325 (2005).
- Myong, S., Bruno, M. M., Pyle, A. M. & Ha, T. Spring-loaded mechanism of DNA unwinding by hepatitis C virus NS3 helicase. *Science* **317**, 513–516 (2007).
- Sun, B. *et al.* Impediment of *E. coli* UvrD by DNA-destabilizing force reveals a strained-inchworm mechanism of DNA unwinding. *EMBO J.* **27**, 3279–3287 (2008).
- Dessinges, M. N., Lionnet, T., Xi, X. G., Bensimon, D. & Croquette, V. Single-molecule assay reveals strand switching and enhanced processivity of UvrD. *Proc. Natl Acad. Sci. USA* **101**, 6439–6444 (2004).
- Chemla, Y. R. *et al.* Mechanism of force generation of a viral DNA packaging motor. *Cell* **122**, 683–692 (2005).
- Tsay, J. M., Sippy, J., Feiss, M. & Smith, D. E. The Q motif of a viral packaging motor governs its force generation and communicates ATP recognition to DNA interaction. *Proc. Natl Acad. Sci. USA* **106**, 14355–14360 (2009).
- Singleton, M. R., Sawaya, M. R., Ellenberger, T. & Wigley, D. B. Crystal structure of T7 gene 4 ring helicase indicates a mechanism for sequential hydrolysis of nucleotides. *Cell* **101**, 589–600 (2000).
- Patel, S. S., Rosenberg, A. H., Studier, F. W. & Johnson, K. A. Large scale purification and biochemical characterization of T7 primase/helicase proteins. Evidence for homodimer and heterodimer formation. *J. Biol. Chem.* **267**, 15013–15021 (1992).
- Mathews, C. K. Biochemistry of deoxyribonucleic acid-defective amber mutants of bacteriophage T4. 3. Nucleotide pools. *J. Biol. Chem.* **247**, 7430–7438 (1972).
- Hingorani, M. M. & Patel, S. S. Interactions of bacteriophage T7 DNA primase/helicase protein with single-stranded and double-stranded DNAs. *Biochemistry* **32**, 12478–12487 (1993).
- Liao, J. C., Jeong, Y. J., Kim, D. E., Patel, S. S. & Oster, G. Mechanochemistry of T7 DNA helicase. *J. Mol. Biol.* **350**, 452–475 (2005).
- Crampton, D. J., Mukherjee, S. & Richardson, C. C. DNA-induced switch from independent to sequential dTTP hydrolysis in the bacteriophage T7 DNA helicase. *Mol. Cell* **21**, 165–174 (2006).
- Yu, X., Hingorani, M. M., Patel, S. S. & Egelman, E. H. DNA is bound within the central hole to one or two of the six subunits of the T7 DNA helicase. *Nature Struct. Biol.* **3**, 740–743 (1996).
- Enemark, E. J. & Joshua-Tor, L. Mechanism of DNA translocation in a replicative hexameric helicase. *Nature* **442**, 270–275 (2006).
- Thomsen, N. D. & Berger, J. M. Running in reverse: the structural basis for translocation polarity in hexameric helicases. *Cell* **139**, 523–534 (2009).

**Supplementary Information** is linked to the online version of the paper at [www.nature.com/nature](http://www.nature.com/nature).

**Acknowledgements** We thank members of the Wang laboratory for critical reading of the manuscript. We also thank M. A. Hall for assistance with single-molecule assays, data acquisition and data analysis. We wish to acknowledge support from National Institutes of Health grants (GM059849 to M.D.W.; GM55310 to S.S.P.), National Science Foundation grant (MCB-0820293 to M.D.W.) and Cornell's Molecular Biophysics Training Grant (T32GM008267) Traineeship (to D.S.J. and B.Y.S.).

**Author Contributions** B.S., D.S.J., S.S.P. and M.D.W. designed the experiments. D.S.J. found the helicase slippage with ATP. B.S. carried out all single-molecule work and, together with B.Y.S., analysed and interpreted single-molecule data. G.P. performed all the ensemble experiments. M.P. and G.P. purified and analysed the wild-type and mutant T7 gp4 proteins. M.D.W. formulated the theoretical models. B.S., D.S.J., B.Y.S., S.S.P. and M.D.W. wrote the manuscript.

**Author Information** Reprints and permissions information is available at [www.nature.com/reprints](http://www.nature.com/reprints). The authors declare no competing financial interests. Readers are welcome to comment on the online version of this article at [www.nature.com/nature](http://www.nature.com/nature). Correspondence and requests for materials should be addressed to M.D.W. ([mwang@physics.cornell.edu](mailto:mwang@physics.cornell.edu)) or S.S.P. ([patells@umdndj.edu](mailto:patells@umdndj.edu)).

## METHODS

**Protein and DNA preparations.** Wild-type T7 helicase (gp4A') and Y535F 4A' were expressed and purified as described previously<sup>17</sup>. A 5.2 kb DNA was constructed as described elsewhere<sup>9,25</sup>, with minor modifications. Briefly, a ~1.1 kb anchoring segment was prepared by PCR from pRL574 using a digoxigenin-labelled primer, and then digested with BstXI (NEB) to produce a 3 bp overhang. A ~4.1 kb unzipping/translocation/unwinding segment was derived from pCP681 by digestion with EarI (NEB) and ligated to a biotin-labelled 37 bp segment lacking a 5' phosphate on the distal end. The anchoring segment and unzipping segment were then ligated, with a nick due to the missing phosphate. For ssDNA translocation experiments (Supplementary Fig. 8), the ~4.1 kb segment was capped with a hairpin (5'-TAGGGCGACCTAGCTCTATGCTAGGTCGCC-3').

**Single-molecule assays.** Sample preparation was similar to that previously described<sup>9</sup>. Briefly, helicase was prepared by first incubating 2  $\mu\text{M}$  of the helicase monomer for 20 min in the unwinding buffer. This solution was then further diluted to obtain the final experimental concentration of helicase monomer, nucleotides and  $\text{MgCl}_2$ . DNA tethers were formed by first non-specifically coating the sample chamber surface with anti-digoxigenin (Roche), followed by an incubation with digoxigenin tagged DNA. Streptavidin-coated 0.48  $\mu\text{m}$  polystyrene microspheres were then added to the chamber. Finally, helicase solution was flowed in just before data acquisition. The helicase unwinding buffer was 20 mM Tris-HCl (pH 7.5), 3 mM EDTA, 0.02% Tween 20, 50 mM NaCl, NTPs or dNTPs at the concentrations specified in the text, and  $\text{MgCl}_2$  at a concentration 5 mM in excess of the total nucleotide concentration (Supplementary Fig. 13). The helicase monomer concentration was adjusted between 1–500 nM for each buffer condition so that the average unwinding initiation time (defined as the time between when the DNA was initially mechanically unzipped and when the helicase began to unwind) was approximately the same for all experiments (Supplementary Fig. 3).

Experiments were conducted in a climate-controlled room at a temperature of 23.3  $^{\circ}\text{C}$ , but owing to local laser trap heating the temperature increased slightly to  $25 \pm 1^{\circ}\text{C}$  (ref. 26). Each experiment was conducted in the following steps (Supplementary Fig. 1). First, several hundred base pairs of dsDNA were mechanically unzipped, at a constant velocity of  $1,400 \text{ bp s}^{-1}$ , to produce a ssDNA loading region for helicase. Second, after the force dropped owing to helicase loading and initiation of unwinding, several hundred more base pairs were mechanically unzipped to generate ssDNA for helicase translocation. Third, the fork position was maintained until the force dropped again, indicating that the helicase had again reached the junction, at which point the force was allowed to drop to

8 pN and then maintained at this level as helicase unwound the remaining ~3 kb of dsDNA. Measurements of ssDNA translocation rates and dsDNA unwinding rates by T7 helicase were thus obtained for each tether.

**Data collection and analysis.** Data were low-pass filtered to 5 kHz and digitized at 12 kHz, then were further averaged to 110 Hz. The acquired data signals were converted into unwound base pairs as previously described<sup>9,25</sup>. To improve positional accuracy and precision, the data were then aligned to a theoretical unzipping curve for the mechanically unzipped section of the DNA<sup>27</sup>. Slippage events were identified by a threshold on the instantaneous unwinding rate at each sequence position (Supplementary Fig. 4). We used a threshold of  $2,000 \text{ bp s}^{-1}$  in the reverse velocity for identifying slippage. Unwinding rates from each trace were found from linear fits to the unwinding between adjacent slippage events. An average unwinding rate was obtained from a number of traces. Distances travelled between slips were compiled to determine processivity. These distances followed an exponential distribution, indicating a stochastic process in slippage<sup>28</sup>. Processivity is defined as the mean distance of the distribution (Supplementary Fig. 4b).

**Modeling.** If dTTP and ATP compete for binding to helicase according to the kinetic pathway outlined in Fig. 2d, then the resulting unwinding rate is:  $V_{\text{tot}} = \left( V_{\text{max}}^{\text{ATP}} \frac{[\text{ATP}]}{K_{\text{M}}^{\text{ATP}}} + V_{\text{max}}^{\text{dTTP}} \frac{[\text{dTTP}]}{K_{\text{M}}^{\text{dTTP}}} \right) / \left( 1 + \frac{[\text{ATP}]}{K_{\text{M}}^{\text{ATP}}} + \frac{[\text{dTTP}]}{K_{\text{M}}^{\text{dTTP}}} \right)$ , where for each type of nucleotide  $K_{\text{M}} = \frac{k_{-1} + k_2}{k_1}$  and  $V_{\text{max}} = sk_2$  with  $s$  being the step size (in nucleotides) (see Supplementary Discussion). In the presence of dTTP and ATP, if  $n$  helicase subunits coordinate in their chemo-mechanical activities and DNA binding, then the resulting distance between slips (processivity) is:  $d_{\text{processivity}} = c \left( V_{\text{max}}^{\text{ATP}} \frac{[\text{ATP}]}{K_{\text{M}}^{\text{ATP}}} + V_{\text{max}}^{\text{dTTP}} \frac{[\text{dTTP}]}{K_{\text{M}}^{\text{dTTP}}} \right) / \left( \frac{[\text{ATP}]/K_{\text{M}}^{\text{ATP}}}{[\text{ATP}]/K_{\text{M}}^{\text{ATP}} + [\text{dTTP}]/K_{\text{M}}^{\text{dTTP}}} \right)^{n-1}$  (Supplementary Discussion), with  $c$  being a proportionality constant. This expression was used to fit data in Fig. 3b, c with  $c$  and  $n$  as fit parameters.

- Koch, S. J., Shundrovsky, A., Jantzen, B. C. & Wang, M. D. Probing protein-DNA interactions by unzipping a single DNA double helix. *Biophys. J.* **83**, 1098–1105 (2002).
- Peterman, E. J., Gittes, F. & Schmidt, C. F. Laser-induced heating in optical traps. *Biophys. J.* **84**, 1308–1316 (2003).
- Shundrovsky, A., Smith, C. L., Lis, J. T., Peterson, C. L. & Wang, M. D. Probing SWI/SNF remodeling of the nucleosome by unzipping single DNA molecules. *Nature Struct. Mol. Biol.* **13**, 549–554 (2006).
- Lohman, T. M., Tomko, E. J. & Wu, C. G. Non-hexameric DNA helicases and translocases: mechanisms and regulation. *Nature Rev. Mol. Cell Biol.* **9**, 391–401 (2008).